Some Experimental Results on Sphere and Disk Drag

FREDERICK W. ROOS*
McDonnell Douglas Corporation, St. Louis, Mo.
AND
WILLIAM W. WILLMARTH†
The University of Michigan, Ann Arbor, Mich.

The drag on spheres and disks moving rectilinearly through an incompressible fluid has been measured for Reynolds numbers (Re) from 5 to 100,000. Test models were mounted on a carriage which rode along a linear air bearing track system. Tests were performed by towing the models through a channel filled with glycerine-water mixtures. Forces and moments on the models were sensed by strain gage transducers; hydrogen bubble flow visualization was utilized in relating these forces to the unsteady wake flows. Steady drag results agreed with existing data except for the disk at $100 < Re < 1000$, in which the drag coefficient values were up to 50% below the level of existing data; drag force unsteadiness during steady motion was always <5% for the sphere and <3% for the disk. Sphere drag measurements under constant acceleration from rest showed the apparent mass concept to be valid (at high Re) until the sphere had traveled approximately one diameter, after which the quasi-steady drag (based on instantaneous velocity) showed good agreement with the actual drag. Interference effects of the sting supports used in these tests are discussed.

Nomenclature

a = acceleration in direction of motion
C_D = $S/(\frac{1}{8}\pi\rho U^2 d^2)$, the drag coefficient
d = diameter of sphere or disk
D = drag force
L = lift force
Re = Ud/ν, the Reynolds number
S = side force
t = time
U = translational speed of sphere or disk
α = angle of attack
ν = kinematic viscosity of fluid
ρ = fluid density

Introduction

INTEREST in the behavior of a sphere or disk moving through a fluid goes back many years. The first recorded measurements related to sphere drag were published by Sir Issac Newton; a multitude of studies of sphere and disk aerodynamics has followed. Many of these were noted by Torobin and Gauvin[1] in their comprehensive review of sphere aerodynamics.

Recently, several aerospace-oriented engineering problems have arisen which have prompted renewed interest in sphere and disk aerodynamics. One such example is the problem of accelerated two-phase flow through rocket nozzles, reviewed a short time ago by Hoglund.[2] Another example is the uncertainty introduced by aerodynamically induced oscillations of balloons used to measure the vertical profile of atmospheric winds.[3] In addition to such specific problems, the lack of understanding of bluff-body flows in general has been responsible for continued study of sphere and disk flows.

In spite of the many investigations into sphere and disk aerodynamics, even the basic steady-flow relationships between drag coefficient and Reynolds number (C_D and Re, respectively) for these two bodies are somewhat indefinite, i.e., the scatter in existing data amounts to at least 10% over much of the Re range.[4] The situation is considerably more uncertain in the case of accelerated motion. A further difficulty with existing experimental data for Re less than about 1000 is that all of them were obtained in free-fall (or free-rise) tests; consequently the effects of coupling of the body dynamics with the unsteady wake processes were involved.

An attempt to clarify some of the remaining uncertainties in the aerodynamics of spheres and disks, particularly the unsteady features, was recently undertaken.[4] The research program, which was entirely experimental because of the extreme mathematical complexity of the problem, was primarily intended to be an exploration, at low Re, of the relationship between wake unsteadiness and the fluctuating transverse forces and moments acting on the sphere or disk. The experiment achieved only limited success, as it was discovered that the sting-type model support, an indispensable part of the test apparatus, tended to stabilize the wake and to interfere with the unsteady vorticity-shedding process at low Re. Nevertheless, it is felt that the longitudinal force (drag) measurements were essentially correct, and it is with the sphere and disk drag data alone that this paper is concerned.

Experimental Equipment

A detailed description of the experiment and equipment can be found elsewhere.[4] The setup, sketched in Fig. 1, consisted of a 0.61- × 0.61- × 9.75-m plywood and fiber glass towing channel, above which was suspended a linear air bearing track system. Air bearings were selected over conventional rail-type tracks because they offered a potentially shock- and vibration-free linear motion; prior experience with wheel-on-rail systems had shown the great difficulty involved in trying to obtain a satisfactorily low vibration level with track systems. The 9.75-m-long air bearing system employed in these tests consisted of a V groove bearing (made by joining three commercially available bearing units end to end) for tracking and a parallel flat-surface bearing (built in-house from a 5.08 cm square aluminum tube, 0.318-cm wall) for stability. Adjacent to the track system was a loop of cable that could be driven at various speeds, forward and reverse, by a controllable electric motor drive unit. Attached to the cable was a carriage from which the strain-gage-instrumented test model

Received February 11, 1970; revision received August 31, 1970. This research was supported by a grant from the U.S. Army Research Office (Durham); the results noted here formed part of the first author's doctoral dissertation in The University of Michigan.

* Research Scientist, Fluid Mechanics Group, McDonnell Douglas Research Laboratories. Member AIAA.
† Professor of Aerospace Engineering. Member AIAA.

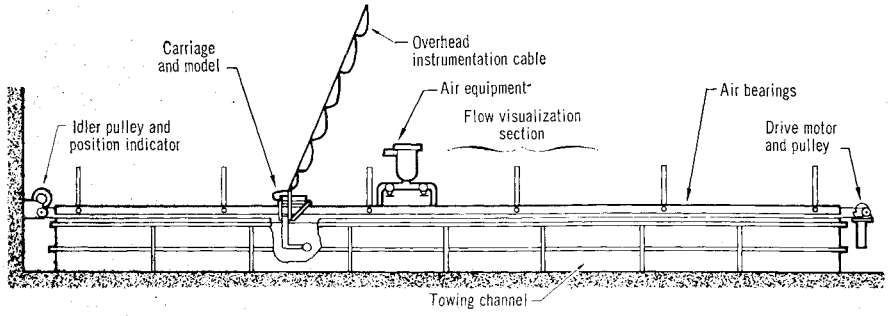

Fig. 1 Schematic of towing channel installation.

(7.62-cm diam sphere or disk) was suspended, and on which was mounted a package of solid-state amplifiers for amplifying and modifying the strain gage signals. Figure 2 shows details of the track and carriage arrangements.

To facilitate the study of a wide range of *Re*, glycerine-water mixtures were employed as the working fluid. A section of the towing channel was equipped with lights and electrodes for hydrogen bubble flow visualization in the channel fluid.[5] Flow visualization was used to permit study of the relationship between wake fluctuations and the variations of forces on the test model.

Constant-speed runs were accomplished by starting the drive system, rapidly accelerating it to run speed, holding run speed for the test, and then decelerating quickly to a stop. For studies of accelerated motion, the carriage was detached from the drive system and connected to a long spring, which was stretched out parallel to the track to provide the accelerating force.

An overhead instrumentation cable connected the strain gage amplifiers to the external electronic gear. Analog feedback amplifiers were used to form appropriate combinations of data signals when this was necessary, e.g., to compensate for strain gage balance interactions. Finally, the output signals were recorded on a strip chart recorder for later analysis.

Results

Sphere at Constant Velocity

Steady sphere drag was measured through most of the range $5 < Re < 100{,}000$. These data, in coefficient form, are given in Table 1 and are also plotted in Fig. 3, where they are superimposed on a band representing the variation shown by existing, reliable sphere drag coefficient data.[6–13] The general over-all agreement serves both to further verify the existing data and to indicate the accuracy of the experiment.

The greatest scatter in the present data occurs at high subcritical *Re* (5500–100,000), where it also appears that the C_D values are somewhat higher over-all than the existing data level. The probable explanation of this feature is that almost all of the present data in this *Re* range were obtained in what amounted to a shakedown test of the experimental apparatus. Considerable mechanical vibration existed in the carriage and drive system at that time, resulting in drag force records that were difficult to evaluate with accuracy, particularly at low drag force levels (i.e., at the lower values of *Re* within

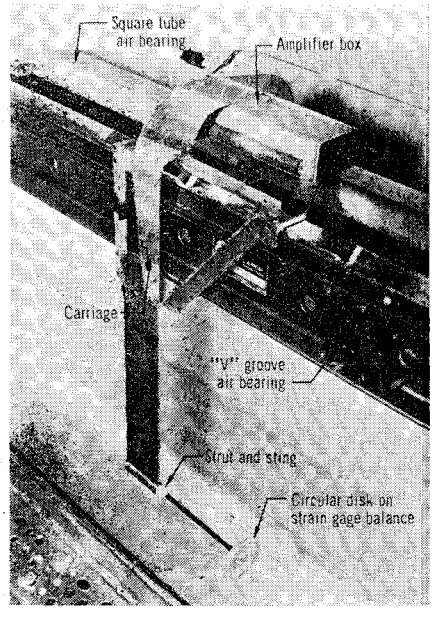

Fig. 2 Photograph of carriage and model assembly on air bearings.

Table 1 Sphere drag coefficient data

Re	C_D	*Re*	C_D	*Re*	C_D
5.33	7.06	286	0.675	6900	0.460
5.99	6.41	311	0.592	7280	0.430
11.0	4.01	312	0.607	7520	0.435
13.1	3.76	318	0.656	8230	0.429
13.2	3.66	358	0.627	8580	0.390
13.9	3.59	361	0.600	8700	0.490
14.6	3.41	364	0.632	9620	0.490
16.2	3.29	379	0.595	13300	0.460
21.1	2.82	409	0.579	13400	0.480
23.4	2.48	444	0.585	13900	0.400
29.1	2.28	468	0.578	14700	0.460
45.0	1.79	472	0.566	16800	0.452
50.6	1.58	480	0.572	18000	0.510
54.4	1.52	500	0.547	18700	0.523
68.9	1.35	522	0.544	19500	0.500
68.9	1.33	532	0.543	21200	0.509
78.2	1.27	532	0.556	23100	0.511
88.1	1.12	557	0.552	23600	0.529
93.8	1.03	579	0.523	23700	0.455
101	1.08	588	0.520	24100	0.524
104	1.05	603	0.531	24200	0.520
108	1.02	644	0.525	25000	0.519
109	1.03	713	0.505	28000	0.495
124	0.994	727	0.480	31900	0.500
130	0.927	833	0.485	32400	0.479
138	0.907	932	0.472	33800	0.457
163	0.879	984	0.466	35400	0.482
168	0.799	985	0.477	35500	0.504
170	0.819	985	0.485	38200	0.513
186	0.799	1000	0.472	41800	0.485
186	0.841	1000	0.483	45900	0.467
189	0.778	1070	0.452	46800	0.468
190	0.751	1330	0.436	52400	0.503
191	0.799	1650	0.440	53500	0.497
193	0.732	1690	0.435	57500	0.480
229	0.711	1950	0.427	57700	0.492
229	0.710	2000	0.430	71900	0.451
240	0.700	5570	0.460	89000	0.502
258	0.721	5990	0.430	100000	0.467
280	0.674	6210	0.390	118300	0.476
284	0.646	6250	0.451		

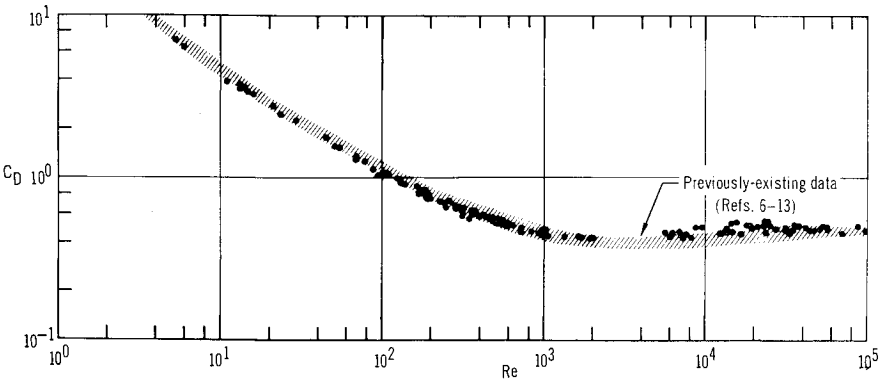

Fig. 3 Mean sphere drag coefficient data from these experiments.

this range). The experience gained in this early testing led to significant refinement of the experimental equipment.

Some scatter also exists in the rest of the data, although no consistent deviation from the previously existing data is evident here. A noteworthy feature of these data is the reduced scatter of points for $400 \leq Re \leq 2000$. Data in this range were obtained with an improved strain gage balance designed especially for the sphere model, whereas the rest of the data in Fig. 3 came from tests with the sphere mounted on the original (sphere and disk) balance.

It is interesting to observe that the sphere C_D-Re data give no indication of the Re at which wake unsteadiness commences, i.e., the data do not show any "jump" or "bend" to mark the onset of wake fluctuations. Actually, the minimum Re for unsteadiness in these tests (with the sting-mounted sphere) was approximately 290; flow visualization tests of the sphere with no sting (accomplished by weighting the sphere and suspending it on two fine threads) showed $Re_{min} \approx 215$. Obviously, the sting support had a significant stabilizing effect on the sphere wake. However, this does not affect the agreement of the present C_D data with those of other workers.

An attempt was made to study the unsteady component of sphere drag during constant velocity motion. In all cases of steady motion, the drag fluctuation was no more than about 5% of the average drag, regardless of whether or not vortex shedding occurred. This, of course, does not include the early stages of accelerated motion (with consequent wake buildup), where large drag fluctuations sometimes existed. The magnitude of the first two or three fluctuations in drag depended greatly on the acceleration imparted to the sphere at the start of a run. In general, more impulsive starts produced greater fluctuations.

Once the sphere wake had built up to its quasi-steady configuration (usually after two or three cycles of vortex shedding), the drag unsteadiness remained slight and did not demonstrate a clear relationship to the vortex shedding process. Figure 4 is a copy of the strip chart record of drag (D) and side force (S) from a typical test run at $Re = 532$.‡ Despite the large fluctuations in S, which flow visualization has shown to correspond to vigorous unsteadiness in the sphere wake, very little related unsteadiness appears in D. In fact, the variation in D is small enough that it may have been due entirely to mechanical unsteadiness in the experimental apparatus. Other run records have been obtained which display even less D fluctuation (at similar Re) than appears in Fig. 4.

A noteworthy feature of the run data in Fig. 4 is the gross difference in the nature of the development of unsteadiness in D and S. The drag force had built up to its maximum value and passed through three cycles of oscillation before S had developed its first (and largest) significant peak. This feature, a characteristic of all data records in which D was combined with either S or L (lift), indicates that the first few cycles of vorticity shedding in the sphere wake must be axially symmetrical and are apparently unrelated to the lateral wake oscillations which develop later in the process of vortex loop shedding.

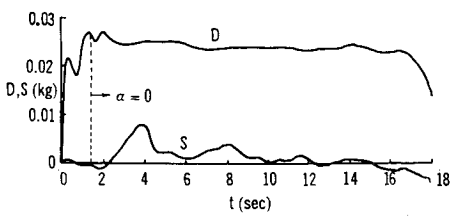

Fig. 4 Reproduction of typical sphere drag data record from run at $Re = 532$.

‡ High-frequency oscillations, which were definitely attributable to vibrations of the carriage, drive, and model mounting, have been filtered out of these data.

Sphere in Accelerated Motion

Several test runs were made in which an accelerometer was mounted on the carriage to permit the study of sphere drag during accelerated motion. A data record from one such test run is given in Fig. 5.

The run which produced the data of Fig. 5 was made in water so that high Re was reached: the maximum value of Re, corresponding to the instant when the acceleration (a) passed through zero, was 66,000. Instantaneous sphere velocity was evaluated at several times (t) by graphical integration of the a record. Values of Re were computed from these velocities and used to obtain appropriate C_D values from Fig. 3, these in turn being used to calculate the D values making up the dashed curve (labeled "D calculated from steady C_D") in Fig. 5.

Also shown in Fig. 5 is a dotted curve representing D calculated according to the theory proposed by Odar.[14,15] In that theory, the expression for D of a sphere accelerating along a rectilinear path consists of three terms, one of which is just the drag as calculated above, i.e., based on steady state C_D. The other two terms are proportional to a and to a "time-history" function of a, respectively, each of these terms containing a coefficient dependent upon the acceleration modulus

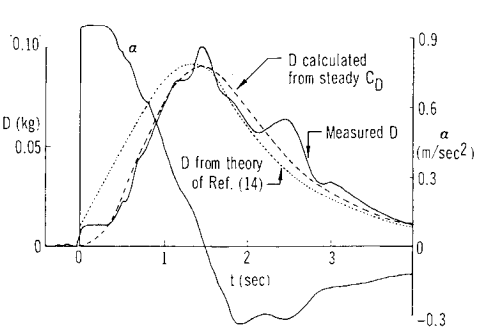

Fig. 5 Data record of sphere drag during acceleration from rest.

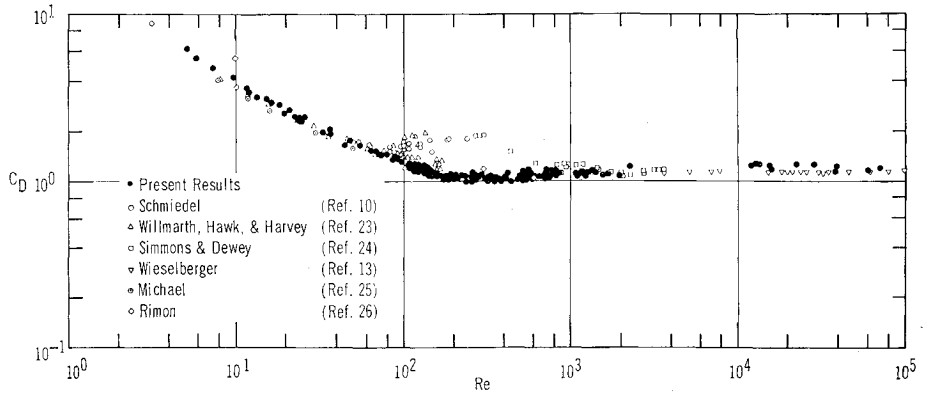

Fig. 6 Steady drag coefficient data for disk normal to flow.

$(= U^2/ad)$. Odar[14,15] found these coefficients to be independent of Re for $Re < 200$, and suggested that this might also be so for higher values of Re.

Inspection of the curves in Fig. 5 reveals that the measured D is reasonably well approximated by the steady-state D curve, except during the initial 0.30 sec and at times when the measured D was fluctuating. The curve representing the Odar theory, on the other hand, does not agree well with the measured D except when the acceleration-dependent terms are small, i.e., when $t > 1.5$ sec.

The most interesting portion of Fig. 5 is the startup ($0 < t < 0.30$ sec), where a nonzero flat spot occurs in the measured D. The constant value of D existing during this initial portion of the run, where a is also essentially constant, is within 3% of the D value computed according to the apparent mass concept of potential flow theory.[16] Nearly identical results were obtained from several other test runs in which a_{max} varied from 0.92 to 1.95 m/sec^2; calculations of sphere displacement revealed that the sphere traveled a distance approximately equivalent to one sphere diameter before the region of separated flow had grown large enough to destroy the potential flow pressure distribution about the sphere.

An important comparison can be drawn between the above result and theoretical calculations of the flow about an accelerated sphere. Although no such calculations have been made for the case of constant acceleration, Boltze[17] studied the flow past an impulsively started sphere. Using a boundary-layer type of analysis based on successive approximations to the velocity field about the sphere, a power series in t being assumed for the velocity components, he determined that flow separation would commence at the rear stagnation point on an impulsively started sphere after the sphere had traveled 0.196 of a diameter (d). An estimate of the onset of flow separation for a sphere subject to constant acceleration can be made by considering the corresponding results for a circular cylinder: calculations[18] (employing analytical techniques comparable to Boltze's) show that separation on a cylinder occurs after a travel of $0.26d$ for constant acceleration (of any magnitude) from rest compared to $0.16d$ for an impulsive start. If it is assumed (as a rough guess) that the result for constant acceleration of a sphere bears the same relationship to the impulsive-start result as exists in the case of the cylinder, Boltze's result scales up to $0.32d$ for the distance covered by a constantly accelerating sphere before separation appears. Since the experiment showed that a sphere travels about $1.0d$ before the apparent mass concept becomes invalid, it is evident that considerable growth of the separation bubble must occur before the pressure distribution about the sphere becomes significantly different from the potential flow pressure distribution.

Rimon and Cheng[19] have recently published some numerical results concerning an impulsively started sphere. They report that the sphere moves through a distance of $0.32d$ before separation appears at the rear stagnation point; further, one can discern from their computer-generated streamline pictures that, although the separation bubble rapidly spreads over the rear of the sphere, it does not lengthen appreciably (and thereby distort the outer-flow streamlines) until the sphere has moved on the order of $1.0d$. Although the coincidence of these numbers with those noted previously is accidental,§ the indication is clear that separation first occurs well before the outer flow shows significant alteration.

Acceleration tests similar to those described previously were attempted in a glycerine-water mixture which reduced the maximum value of Re to about 300, but the low values of Re existing during the early stages of these tests runs meant that the vorticity about the sphere diffused so rapidly that no period of potential flow with constant drag force could be observed. Also, incorrect drag compensation¶ precluded the type of quantitative drag comparison shown in Fig. 5.

The other times at which the measured and calculated D values in Fig. 5 differ significantly are undoubtedly related to the shedding of vortices in the sphere wake.** This would correspond to the measurements by Schmidt[20] of the velocity of a sphere dropped from rest in a vertical column of fluid. He found that fluctuations in sphere velocity during acceleration coincided with the shedding of vortex loops.

A similar phenomenon occurred during startup of most of the normal sphere drag test runs: the drag force measured during a rapidly started drag test would exceed, or "overshoot," the steady value. Some drag overshoot is evident in the low Re drag record of Fig. 4, but the effect was much more pronounced in high Re runs, where the overshoot was as much as 30% above the steady drag. Of course, the magnitude of the overshoot also depended on the acceleration of the sphere.

Corresponding phenomena for impulsively started circular cylinders and normal flat plates were recently studied by Sarpkaya.[21] The employment of flow visualization enabled him to relate the drag overshoot to the growth and shedding of the initial vortices.

What evidently happens is that, when the sphere is put into motion very rapidly at high Re, vorticity is slow to diffuse and therefore accumulates rapidly in the growing separation bubble behind the sphere. Although this bubble of trapped vorticity soon reaches unstable proportions, the growth of the bubble is so rapid that the bubble becomes much larger than its quasi-steady-state size before instability succeeds

§ Note that, in fact, the distance-traveled-before-separation number indicated by the work of Rimon and Cheng for an impulsively started sphere agrees better with the present authors' approximate number for the constant acceleration case than it does with Boltze's corresponding number for the impulsive start case!

¶ Drag compensation refers to the use of feedback amplifiers to subtract the force resulting from sphere inertia (proportional to the accelerometer output) from the drag transducer signal to yield aerodynamic drag.

** The flow visualization equipment was not available for these acceleration tests, so positive affirmation of this point was not possible.

in causing a vortex loop to be cast into the wake. During this period, the pressure drag on the sphere rises above its steady-state value both because the surface area covered by the separation bubble is temporarily greater than it ultimately becomes and because the enlarged wake bubble distorts the outer flow, reducing the base pressure below its eventual steady value.

Although sphere deceleration ($a < 0$) was not studied specifically, some observations were made and a few pertinent comments are in order. Lunnon,[22] in writing about an extensive study of accelerating free-fall spheres ($a > 0$) which he conducted several years ago, suggested that C_D with acceleration should be greater than the steady-state value regardless of the sign of a. This cannot be correct. Consider, for example, a sphere moving through a still fluid at constant velocity and with a fully developed wake. The fluid entrained in the wake moves, relative to the undisturbed fluid, in the direction of of sphere motion, but with a lower velocity. If the sphere is brought rapidly to rest, corresponding to large, negative acceleration, the momentum of the fluid in the wake will cause it to wash over the rear surface of the sphere, exerting a force on the sphere in the upstream direction (i.e., a negative drag force—such a force was often observed in these tests when the sphere was stopped at the conclusion of a run). Relating the previous argument to the case of a sphere entrained in a fluid stream, it is clear that for large decelerations C_D can be significantly lower than the steady-state C_D owing to the sphere being accelerated into its own wake.

Disk at Constant Velocity

Coefficients of steady drag for a circular disk were measured through most of the range $5 < Re < 70{,}000$. The results of these measurements are presented in C_D vs Re form in Table 2 and in Fig. 6, where they are compared with all available experimental[10,13,23,24] and theoretical[25,26] disk C_D data. The most obvious feature of Fig. 6 is the disagreement between the new data and existing experimental data for $100 < Re < 1000$. This lack of agreement stems in part from the fact that much of the previous experimental data in this Re range were obtained with falling disks that were free to oscillate in pitch, whereas the disk used in the tests reported here was rigidly constrained to one-dimensional motion. The close agreement between the free-fall data of Schmiedel[10] and the wind-tunnel data of Simmons and Dewey,[24] which for a long time led to the belief[27] that the disk C_D curve had a "bump" in it in this Re range, is believed to be fortuitous. Regarding the wind tunnel disk data of Simmons and Dewey,[24] it should be mentioned that they were rather skeptical of their low Re data, stating that "it is doubtful whether the observed drag was accurate to within twenty percent" at the lowest Re ($= 282$) of their tests.

The cause of the increase in apparent C_D as a result of pitching oscillation of a disk is not clearly understood. A possible explanation rests in the fact that disks free to oscillate in pitch usually undergo lateral translational oscillations as well.[23] When this occurs, the apparent speed of the disk along its mean (i.e., straight-line) path is lower than the true speed of the disk along its actual trajectory, and consequently a value of C_D based on the apparent speed will be greater than the true average C_D. Since the normal force coefficient for a disk might reasonably be expected to be independent of angle of attack (α) for $\alpha > 35°$–$40°$, as Hoerner[27] shows it to be at higher Re, the true average C_D for moderate-amplitude oscillations†† ought not to be much smaller than C_D for a non-oscillating disk at the same Re. If this is so, and if the actual disk trajectory is noticeably longer than the corresponding vertical distance of fall, then a C_D determination based upon apparent (vertical) speed could very easily yield inflated C_D values. (In this connection, it should be noted that most free-fall test data, including specifically those of Schmiedel,[10] were analyzed in terms of an average vertical speed.) A crude kinematic analysis of the motion of a falling disk appears to bear out the preceding argument, but is too rough and too lengthy to warrant inclusion here.

It is interesting to compare the present experimental drag data with the numerical results of Michael[25] and Rimon.[26] The Rimon data (at Re values of 10, 100, 300, and 600) show C_D decreasing monotonically with increasing Re (i.e., a "bump" is not indicated), but do not fit the experimental curve. It appears that reducing all Rimon's Re values by one-half would put his calculated drag coefficients right on the experimental data, but whether or not the Re values are responsible for the discrepancy is unknown. Michael's computed results, on the other hand, agree well with the experimental data, appearing to be just a bit low. However, neither numerical computation seems to be fully correct. This can be seen in the streamline patterns produced by the computer calculations. As has been noted before,[4,26] the Michael calculation errs in predicting that separation occurs first at the rear stagnation point rather than at the disk edge. Rimon's calculation is satisfactory on this score, but it produces separation bubbles that are (at a given Re) too short. This is evident when one compares his result for $Re = 100$ with the flow photograph presented by Willmarth et al.[28] at approximately the same Re.

Table 2 Disk drag coefficient data

Re	C_D	Re	C_D	Re	C_D
5.06	6.22	131	1.18	530	1.14
5.76	5.44	131	1.14	530	1.08
7.23	4.80	132	1.17	535	1.03
9.48	4.27	136	1.14	555	1.17
11.7	3.68	138	1.21	572	1.14
12.0	3.45	142	1.15	586	1.02
13.3	3.24	142	1.09	590	1.02
15.0	3.16	142	1.16	594	1.03
16.1	2.99	148	1.09	645	1.06
18.0	2.88	156	1.07	673	1.06
19.3	2.59	158	1.08	697	1.04
20.9	2.69	169	1.07	707	1.18
22.3	2.48	173	1.02	711	1.11
24.2	2.45	174	1.02	722	1.15
24.2	2.35	178	1.08	722	1.04
24.5	2.33	186	1.01	745	1.08
25.5	2.47	191	1.09	746	1.14
32.5	2.00	199	1.01	771	1.12
35.6	2.05	205	1.06	800	1.12
36.2	1.97	209	1.07	803	1.14
43.9	1.66	229	1.08	808	1.09
46.7	1.78	231	1.06	1020	1.10
54.2	1.68	255	1.06	1030	1.07
64.0	1.53	256	1.13	1130	1.11
68.0	1.53	270	1.04	1140	1.11
71.4	1.47	270	1.02	1180	1.07
72.2	1.44	279	1.04	1180	1.08
79.0	1.44	290	1.09	1320	1.11
79.1	1.38	309	1.02	1540	1.08
87.1	1.38	309	1.01	1660	1.09
91.8	1.36	312	1.01	2250	1.18
97.3	1.30	314	1.02	9020	1.20
107	1.27	325	1.03	12000	1.24
108	1.24	353	1.00	12700	1.28
108	1.28	358	1.04	13000	1.28
117	1.23	374	1.02	15300	1.24
117	1.21	383	1.00	16000	1.19
117	1.20	384	0.994	22400	1.27
117	1.25	409	1.07	28800	1.27
117	1.23	420	1.12	38200	1.24
121	1.15	436	1.00	38700	1.15
122	1.25	481	1.02	50100	1.16
123	1.21	494	1.08	60400	1.17
131	1.23	517	1.01		

†† Note that α will oscillate about a 90° mean value.

A further interesting feature of the data in Fig. 6 is the rather abrupt flattening out of the C_D–Re curve as Re is increased into the range where wake unsteadiness occurs. (Minimum Re for disk wake unsteadiness in these tests was about 160; the discrepancy between this value and the value $Re_{min} \approx 100$ noted by others[23,24] is attributed to sting influence.) This "bend" in the disk drag curve contrasts with the sphere drag results noted previously. Although a full explanation of this feature of the disk C_D data is lacking, the difference between the sphere and disk C_D curves is understandable in light of some flow visualization results. Observations of sphere and disk wakes at Re slightly above the minimum Re for unsteadiness revealed that the fluctuations in the sphere wake appeared first at the "tail" of the separation bubble, involving more of the bubble at higher Re. On the other hand, the fluctuations in the disk wake always involved fluid in the vicinity of the disk. From these results, it is not difficult to argue that the onset of wake unsteadiness has a greater effect on C_D for the disk.

The primary factor in the general scatter of the data is the rather poor repeatability of the disk drag transducer; this was pointed out previously in the discussion of sphere drag results.

As was the case with the sphere, the disk drag results for $9000 \leq Re \leq 70{,}000$ were obtained early in the course of the research. Considerable mechanical vibration existed in the experimental apparatus at the time, and this showed up in the drag records from these early tests. The resultant uncertainty in the determination of D is probably responsible for the apparently high values of C_D.

As in the sphere tests, drag fluctuations were not significant in the disk drag tests. Except for the large fluctuations during the wake development period, very little fluctuation existed in D even when vortex loop shedding occurred. Analysis of many disk drag data records showed that, during the steady-state portion of a test run, the drag fluctuations never exceeded 3% of D.

Wall Interference Effects

Although wall effects were not investigated during the course of the experiments reported here, and the data herein were not corrected for wall interference, several efforts reported in the literature have focused on the problem. For example, Fidleris and Whitmore[28] performed an extensive, careful study of wall effects on the drag of falling spheres; their results show that, for the blockage ratio of the present experiments (sphere- or disk-to-channel cross-section ratio = 0.012), wall interference produces a drag increase ranging from close to 10% at $Re = 10$ to less than 2% for $Re \geqq 100$. Of course, these figures serve only to provide an estimate of the magnitude of the wall effect, because of the geometry difference (square channel cross-section as opposed to circular cylinders used by Fidleris and Whitmore) and the existence of a streamwise free surface in the tests reported here.‡‡ Regarding the unsteady features of the sphere flow field, Möller[29] determined that increasing the proximity of bounding walls stabilized the sphere wake, i.e., increased the Re corresponding to a particular wake configuration, but otherwise did not substantially alter the dynamic processes of the flow. Finally, a theory developed by Maskell[30] is applicable to the problem of wall influence on the drag of a disk. His work shows that, for $Re > 100$, the presence of confining walls raises the disk drag by less than 5% (for the blockage ratio of the present tests). Again, this number cannot be applied directly to the results reported here because of the free surface on the towing channel.

‡‡ Incidentally, the observation was made that free surface distortion did not contribute significantly to the drag values measured during the experiments reported herein.

Conclusions

Though many questions regarding bluff-body flows remain to be answered, the series of sphere and disk flow studies reported here has produced new information to assist in the understanding of these unsteady flows. Specific conclusions resulting from this work are 1) sphere drag measurements in the range $5 < Re < 100{,}000$ agreed closely with previously existing data; 2) results for the drag on a circular disk reproduced existing data except for $100 < Re < 1000$: in this range the measured C_D for the nonoscillating disk was as much as 50% smaller than that indicated by existing data; 3) the drag on a sphere or disk moving rectilinearly at constant speed is not significantly affected by vortex shedding in the wake; maximum drag unsteadiness was less than 5% of the total drag on the sphere and less than 3% of the total disk drag; 4) drag on a sphere accelerated from rest to a constant velocity exceeds the steady-state drag by as much as 30% at high Re, until the final quasi-steady wake configuration becomes established; 5) the potential flow apparent mass concept is valid for the first diameter of motion of a sphere undergoing constant acceleration such that $Re \approx 30{,}000$ when the sphere has moved one diameter; beyond this point, the drag is reasonably well approximated by the steady-state drag corresponding to the instantaneous sphere velocity.

References

[1] Torobin, L. B. and Gauvin, W. H., "Fundamental Aspects of Solids-Gas Flow, Part I: Introductory Concepts and Idealized Sphere Motion in Viscous Regime," *The Canadian Journal of Chemical Engineering*, Vol. 37, No. 4, Aug. 1959, pp. 129–141; also "Part II: The Sphere Wake in Steady Laminar Fluids," Vol. 37, No. 5, Oct. 1959, pp. 167–176; also "Part III: Accelerated Motion of a Particle in a Fluid," Vol. 37, No. 6, Dec. 1959, pp. 224–236; also "Part IV: The Effects of Particle Rotation, Roughness and Shape," Vol. 38, No. 5, Oct. 1960, pp. 142–153; also "Part V: The Effects of Fluid Turbulence on the Particle Drag Coefficient," Vol. 38, No. 6, Dec. 1960, pp. 189–200.

[2] Hoglund, R. F., "Recent Advances in Gas-Particle Nozzle Flows," *ARS Journal*, Vol. 32, No. 5, May 1962, pp. 662–671.

[3] Scoggins, J. R., "Aerodynamics of Spherical Balloon Wind Sensors," *Journal of Geophysical Research*, Vol. 69, No. 4, Feb. 15, 1964, pp. 591–598.

[4] Roos, F. W. and Willmarth, W. W., "An Experimental Investigation of the Unsteady Flows About Spheres and Disks," Rept. 01954-1-T, Dec. 1968, Dept. of Aerospace Engineering, The University of Michigan, Ann Arbor, Mich.

[5] Roos, F. W. and Willmarth, W. W., "Hydrogen Bubble Flow Visualization at Low Reynolds Numbers," *AIAA Journal*, Vol. 7, No. 8, Aug. 1969, pp. 1635–1637.

[6] Allen, H. S., "The Motion of a Sphere in a Viscous Fluid," *Philosophical Magazine*, 5th Ser., Vol. 50, No. 314, Sept. 1900, pp. 323–338; also Vol. 50, No. 316, Nov. 1900, p. 519.

[7] Liebster, H., "Über den Widerstand von Kugeln," *Annalen der Physik*, Vol. 82, No. 4, Feb. 26, 1927, pp. 541–562.

[8] Lunnon, R. G., "Fluid Resistance to Moving Spheres," *Proceedings of the Royal Society*, Ser. A, Vol. 118, April 2, 1928, pp. 680–694.

[9] Maxworthy, T., "Accurate Measurements of Sphere Drag at Low Reynolds Numbers," *Journal of Fluid Mechanics*, Vol. 23, Pt. 2, Oct. 1965, pp. 369–372.

[10] Schmiedel, J., "Experimentelle Untersuchungen über die Fallbewegung von Kugeln und Schieben in reibenden Flüssigkeiten," *Physikalische Zeitschrift*, Vol. 29, No. 17, Sept. 1, 1928, pp. 593–610.

[11] Shafrir, U., "Horizontal Oscillations of Falling Spheres," Rept. AFCRL-65-141, Feb. 1, 1965, Air Force Cambridge Research Labs., U.S. Air Force.

[12] Shakespear, G. A., "Experiments on the Resistance of Air to Falling Spheres," *Philosophical Magazine*, 6th Ser., Vol. 28, No. 167, Nov. 1914, p. 728.

[13] Wieselberger, C., "Weitere Feststellungen über die Gesetze des Flüssigkeits- und Luftwiderstandes," *Physikalische Zeitschrift*, Vol. 23, No. 10, May 15, 1922, pp. 219–224.

[14] Odar, F. and Hamilton, W. S., "Forces on a Sphere Accelerating in a Viscous Fluid," *Journal of Fluid Mechanics*, Vol. 18, Pt. 2, Feb. 1964, pp. 302–314.

[15] Odar, F., "Unsteady Motion of a Sphere Along a Circular Path in a Viscous Fluid," *Transactions of the American Society of Mechanical Engineers, Ser. E: Journal of Applied Mechanics*, Vol. 35, No. 4, Dec. 1968, pp. 652–654.

[16] Lamb, H., *Hydrodynamics*, 6th ed., Dover, New York, 1945, p. 124.

[17] Schlichting, H., *Boundary Layer Theory*, 4th ed., McGraw-Hill, New York, 1960, p. 218.

[18] Goldstein, S., ed., *Modern Developments in Fluid Dynamics*, Vol. 1, Dover, New York, 1965, pp. 181–187.

[19] Rimon, Y. and Cheng, S. I., "Numerical Solution of a Uniform Flow over a Sphere at Intermediate Reynolds Numbers," *The Physics of Fluids*, Vol. 12, No. 5, May 1969, pp. 949–959.

[20] Schmidt, F. S., "Zur beschleunigten Bewegung Kügelformig Körper in Widerstehenden Mitteln," *Annalen der Physik*, Vol. 61, No. 7, April 15, 1920, p. 633.

[21] Sarpkaya, T., "Separated Flow about Lifting Bodies and Impulsive Flow about Cylinders," *AIAA Journal*, Vol. 4, No. 3, March 1966, pp. 414–420.

[22] Lunnon, R. G., "Fluid Resistance to Moving Spheres," *Proceedings of the Royal Society*, Ser. A, Vol. 110, Feb. 1, 1926, pp. 302–326.

[23] Willmarth, W. W., Hawk, N. E., and Harvey, R. L., "Investigations of the Steady and Unsteady Motion of Freely Falling Disks," Rept. ARL 63-176, Oct. 1963, Aerospace Research Labs., Office of Aerospace Research, U.S. Air Force. (This report, with an abridged set of data tables, appeared under a similar title in *The Physics of Fluids*, Vol. 7, No. 2, Feb. 1964, pp. 197–208.)

[24] Simmons, L. F. G. and Dewey, N. S., "Wind Tunnel Experiments with Circular Disks," Repts. and Memo 1334, Feb. 1930, Aeronautical Research Council, England.

[25] Michael, P., "Steady Motion of a Disk in a Viscous Fluid," *The Physics of Fluids*, Vol. 9, No. 3, March 1966, pp. 466–471.

[26] Rimon, Y., "Numerical Solution of the Incompressible Time-Dependent Viscous Flow Past a Thin Oblate Spheroid," Rept. 2955, Jan. 1969, Naval Ship Research and Development Center, Washington, D. C.

[27] Hoerner, S. F., *Fluid-Dynamic Drag*, 1st ed., published by the author, Midland Park, N. J., 1958, pp. 3–15, 3–16.

[28] Fidleris, V. and Whitmore, R. L., "Experimental Determination of the Wall Effect for Spheres Falling Axially in Cylindrical Vessels," *British Journal of Applied Physics*, Vol. 12, Sept. 1961, pp. 490–494.

[29] Möller, W., "Experimentelle Untersuchungen zur Hydrodynamik der Kugel," *Physikalische Zeitschrift*, Vol. 39, No. 2, Jan. 15, 1938, pp. 57–80.

[30] Maskell, E. C., "A Theory of the Blockage Effects on Bluff Bodies and Stalled Wings in a Closed Wind Tunnel," Repts. and Memo 3400, Nov. 1963, Aeronautical Research Council, England.

FEBRUARY 1971 AIAA JOURNAL VOL. 9, NO. 2

Method-of-Characteristics Solution of Rarefied, Monatomic Gaseous Jet Expansion into a Vacuum

S. J. ROBERTSON*
Lockheed Missiles & Space Company, Huntsville, Ala.

AND

D. R. WILLIS†
University of California, Berkeley, Calif.

An analytical investigation was made of rarefied gas flow in an axisymmetric jet exhausting into a vacuum. A set of partial differential equations was derived for a single-component, monatomic gas by taking moments of the Boltzmann equation with the BGK approximation of the collision integral. The truncation of the moment equations was based on the hypersonic approximation. The resulting partial differential equations were solved numerically by the method of characteristics. The accuracy of the analytical technique was verified by making calculations for a spherical source flow expansion and comparing the results with those obtained by a previous investigation. The technique was then applied to the calculation of uniform parallel flow from a Mach 3.0 nozzle exhausting into a vacuum with throat Reynolds numbers of 25 and 100. Noncontinuum effects were found to have little influence on the density and velocity fields for nozzles of throat Reynolds numbers down to at least 25. The temperatures were found to behave in much the same fashion as previously predicted for spherical source flow; i.e., the parallel temperature component approaches a finite "freezing" temperature, and the two perpendicular components continue toward zero.

Nomenclature

A = constant in Eq. (2)
b = distance normal to streamline and axial plane (binormal)
f = distribution function
F = equilibrium distribution function
m = molecular mass
M = Mach number
n = distance normal to streamline in axial plane, also number density
p = pressure = $(p_s + p_n + p_b)/3$; with s,n,b or t subscript, component of pressure or shear stress as indicated by subscript
Q = factor in moment of Boltzmann equation
r = radial distance from nozzle axis, also distance from point source
r^* = sonic radius
R = nozzle exit radius
R_g = gas constant
Re^* = throat Reynolds number
s = distance along streamline

Received February 13, 1970; revision received July 2, 1970. This work was supported by NASA-Marshall Space Flight Center, Contract NAS8-21490.

* Research Specialist, Aeromechanics Department.

† Associate Professor of Aeronautical Sciences. Member AIAA.